Study on the damaged ship motion coupled with damaged flow based on the unified viscous/potential prediction model

Shuxia Bu, *China Ship Scientific Research Center*, bushuxia8@163.com

Min Gu, *China Ship Scientific Research Center*, gumin702@163.com

ABSTRACT

The behaviour of a damaged ship is very complex because of the interaction between the ship motion and the flow inside the damaged compartment. Therefore, a feasible prediction method for the damaged ship stability considering the interactions between the damaged ship and the floodwater is very important. In this paper, one nonlinear time domain unified prediction model for the damaged ship motion is proposed, which combines the advantages of potential theory in calculating ship motion and viscous theory in calculating the floodwater flow. In this unified prediction model, the three-dimensional hybrid time domain panel method which is used to calculate the large amplitude motion of damaged ship and the CFD method which is used to calculate the flow in the compartments are coupled with each other in time domain. Two boundary condition forms for the damaged opening are studied. The unified model is verified by comparing the CFD simulation results with ITTC benchmark model. The research show that the proposed unified model captures both the large amplitude motion and the details of floodwater flow very well. The efficiency of the calculation of damaged ship motion in waves is improved as the mesh quantity for CFD simulation is considerably reduced.

Keywords: *Damaged ship motion coupled with damaged flow, 3D time domain hybrid source method, far-field boundary condition, hatch pressure boundary condition.*

1. INTRODUCTION

The damaged ship stability in waves is very complex and the evaluation of the damage ship motion is a difficult task. The performance of a damaged ship in waves is influenced not only by waves but also by the internal loads of the fluid flow and sloshing. The inflow of floodwater causes the change of ship parameters (mass, buoyancy, etc.) and the sloshing of liquid inside the damaged compartment. The load generated by the sloshing of liquid will further affect the motion characteristics of the ship. The motion of damaged ship and the damaged floodwater are coupled with each other. Water flowing into the compartment has a significant effect on the ship stability and safety.

Generally, there are three basic problems related to damaged ship motion (ITTC, 2005): ship with zero forward speed moving on the free surface under the excitation of waves; the flooding phenomenon itself, namely the process of water inflow and outflow through damage openings and progressive flooding through internal spaces; the behavior of the accumulated floodwater inside the ship's compartments and its interaction with the ship.

The dynamic performance of damaged ships in waves are constantly changing, which leads to high nonlinearity of the dynamic system. Therefore, an effective method to reproduce the high nonlinearity of the ship motion and the process of the damaged flow is to solve it in time domain. Up to now, many works have been devoted to the study of the damaged ship motion in waves (Jasionowski and Vassalos, 2011; Umeda et al., 2004; Spanos and Papanikolaou, 2007; Van Walree et al., 2007).

The assessment of damaged ship motion is normally based on potential theory. However, the potential theory cannot accurately capture hydrodynamic loads caused by floodwater; sloshing is usually ignored; the internal water surface is assumed to be horizontal or a free-moving plane; the inflow and outflow of water through the damaged opening are calculated by the modified empirical Bernoulli's equation. Furthermore, the roll damping and damping forces due to floodwater are usually calculated by empirical. Some researchers also use shallow water equation to simulate the physical characteristics of the internal flow (Chang et al., 1998; Santos et al., 2006, 2008). Although the improved model can display the nonlinear characteristics of the flow inside the compartment,

yet the method still fails to characterize flow through external (damage) and internal openings.

CFD method is deemed to be a better choice that can offer a detailed description of the dynamic characteristics of flow. Indeed, it has been used by several researchers to study the flooding process of damaged ships (Cho et al., 2006; Nabavi et al., 2006; Strasser, 2010; Gao and Vassalos, 2015). The research prove that CFD is successful to describe the flow and its characteristics pretty well. However, it should be pointed out that it is hard to simulate the entire damaged ship motion only by CFD method due to high computational costs.

The coupling between the damaged ship motion in waves and damaged floodwater is a very complex problem. The in-waves calculations need to consider not only the motions of damaged ship but also the strong non-linear floodwater dynamics as well as progressive flooding. Particularly, despite a number of studies that focused on the relationship between flooding water and the motion response of damaged ship, the effects of flooding dynamics on the motion of a damage ship is not yet clearly understood.

Considering that CFD method can simulate most of the flow characteristics and parameters, potential flow method has a strong advantage in solving seakeeping problems. Therefore, the coupling method of CFD and potential theory can be used to reduce the computational cost on one hand, and to simulate the flow problem more efficiently on the other hand. In this method, CFD is used to simulate the flow in the damaged compartment whilst the potential flow method is used to calculate the forces due to action of waves. Cho et al. (2006) developed a numerical method that can take into account the internal flow, in which the ship motion is solved by the three-dimensional frequency domain panel method, and the internal fluid motion is solved by the modified VOF method, taking into account the effect of sloshing. Gao et al. (2013) simulated the motion of one damaged Ro-Ro ship coupled with damaged flow, in which the ship motion in waves were calculated with use of strip theory and flows inside the damaged compartment were calculated by RANS equation. Hashimoto et al. (2015) simulated the transient behavior of ships by coupling the three-dimensional MPS method with the conventional 2D strip method.

The above inspire us to establish a method that combines CFD and potential theory to investigate the hydrodynamics of floodwater and its effects on the damaged ship motions. Firstly, a unified viscous/ potential prediction model is proposed, in which the three-dimensional time-domain hybrid source method is used for the calculation of damaged ship motion in waves, and viscous CFD method is used for the simulation of floodwater. Two boundary condition forms for damaged opening are introduced. Then the time domain coupling between damaged ship motion and damaged floodwater are simulated based on this method.

2. RESEARCH OBJECT

The ITTC benchmark model for progressive flooding is selected as the research object. The model made available by NAPA and HUT Ship Laboratory provides experimental data for the validation of numerical simulation method (Ruponen et al., 2007). The model is a barge with eight interconnected compartments, as shown in Fig. 1. Its principal dimensions are shown in Table 1.


Figure 1: The shape model of damaged barge.

The damaged compartments are located in the middle of the hull towards the bow of the ship. The compartments and compartment connections are shown in Fig. 2 and Table 2. The damage opening is located at mid-length of the side wall of compartment R21S, 185mm below the waterline. In the study presented in this paper, DB1 and DB2 in the lower compartment are not connected with the upper compartment and therefore they are not flooded during the simulations.

Table 1: Main dimensions of damaged barges and cabins

Items	Values	Items	Values
Length	4m	Vol	1.45m3
Breadth	0.8m	KB	0.27m
Height	0.8m	BM	0.118m
Draft	0.5m	GM	0.11m
Cb	0.906	KG	0.278m
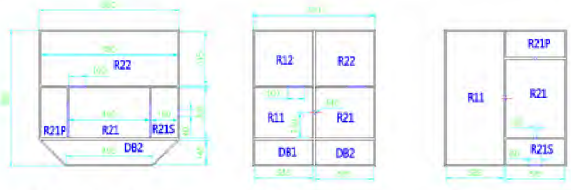
(a) Front view   (b) Side view   (c) Top view
Figure 2: Section diagram of damaged compartment

Table 2: Compartment connections

Opening	Connected compartment	Dimension
FDP	R21↔R21P	20mm×200mm
FDS	R21↔R21S	20mm×200mm
DP	R21↔R11	Φ20mm
SC1	R11↔R12	100mm×100mm
SC2	R21↔R22	100mm×100mm
DAS	R21S↔Sea	60mm×40mm

3. UNIFIED VISCOUS / POTENTIAL PREDICTION MODEL

Mathematical model

Three degrees of freedom (heave-roll-pitch) mathematical model is used for the simulation of damaged ship motion, as follows:

$$(m + A_{33})\ddot{x}_3 + B_{33}\dot{x}_3 + \sum_{j=4,5}\left[A_{3j}\ddot{x}_j + B_{3j}\dot{x}_j\right]$$
$$= F_3^{FK+H} + F_3^{DF} + F_3^{In}$$

$$(I_{44} + A_{44})\ddot{x}_4 + B_{44}\dot{x}_4 + \sum_{j=3,5}\left[A_{4j}\ddot{x}_j + B_{4j}\dot{x}_j\right] \quad (1)$$
$$= F_4^{FK+H} + F_4^{DF} + F_4^{In}$$

$$(I_{55} + A_{55})\ddot{x}_5 + B_{55}\dot{x}_5 + \sum_{j=3,4}\left[A_{5j}\ddot{x}_j + B_{5j}\dot{x}_j\right]$$
$$= F_5^{FK+H} + F_5^{DF} + F_5^{In}$$

where m is the mass of the hull; I_{ii} is the moment of inertia about an i-axis; A_{ij} is the added mass coefficient of the hull; B_{ij} is the damping coefficient of the hull; x_i is the displacement in the i-direction; $\dot{x}_i$ is the velocity in the i-direction; $\ddot{x}_i$ is the acceleration in the i-direction; the roll damping coefficient is calculated based on to the critical rolling damping coefficient:

$$B_{44} = \varsigma \cdot 2\sqrt{(I_{xx} + A_{44})mg} \quad (2)$$

where ς is the critical roll damping coefficient (Ruponen et al., 2007); F_i^{FK+H} is the Froude-Krylov force and hydrostatic force, obtained by integrating the incident wave pressure over the instantaneous wetted surface of the hull; F_i^{DF} is the diffraction

force, integrated over the average wetted surface of the hull; the hydrodynamic coefficients related to radiation force such as A_{ij} and B_{ij} are also integrated over the average wetted surface of the hull; F_i^{In} is the force acting on the interior wall due to floodwater (including sloshing) and incorporating the pressure and shear force generated by viscous flow.

Three Dimensional Hybrid Source Method

Three dimensional time-domain hybrid source method is used for the calculation of damaged ship motions. The field domain is divided into two sub-domains by an arbitrary virtual control surface S_c, as shown in Figure 3. The inner field I is a closed area surrounded by the wetted surface S_b, the partial free surface S_{f1} and the control surface S_c, while the outer field II is a closed area surrounded by the control surface S_c, the remaining free surface S_{f2} and the infinite boundary S_∞ (Bu et al., 2019a, 2019b).
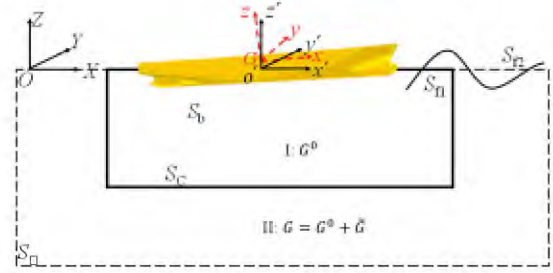

Figure 3: Diagram for the field domains in the three dimensional hybrid source method.

The total perturbation potential in the inner field domains $\Phi_I(P,t)$ satisfies the following conditions in the earth-fixed coordinate system:

$$\nabla^2\Phi_I = 0 \qquad \text{Inner}$$

$$\frac{\partial^2\Phi_I}{\partial^2 t} + g\frac{\partial\Phi_I}{\partial Z} = 0 \quad \text{on } S_{f1},\ t > 0$$

$$\frac{\partial\Phi_I}{\partial\vec{n}} = \vec{V}_n - \frac{\partial\Phi_w}{\partial\vec{n}} \qquad \text{on } S_b,\ t > 0 \qquad (3)$$

$$\Phi_I = \frac{\partial\Phi_I}{\partial t} = 0 \qquad \text{at } t = 0$$

The boundary integral equation of Rankine source in the inner field I can be written as follows:

$$2\pi\Phi_I(P) + \iint_{S_I}(\Phi_I G_n - \Phi_{In}G)dS = 0 \qquad (4)$$

where $\vec{x} = P(X(t), Y(t), Z(t))$ is field point; $\vec{\xi} = Q(\xi(t), \eta(t), \zeta(t))$ is source point; $G = 1/r_{PQ}$ is simple Green function, with r_{PQ} given as:

$$r_{PQ} = |P - Q| = \sqrt{(X - \xi)^2 + (Y - \eta)^2 + (Z - \zeta)^2}$$

The total perturbation potential $\Phi_{II}(P,t)$ satisfies the following conditions in earth-fixed coordinate system:

$$\nabla^2\Phi_{II} = 0 \qquad \text{Outer}$$
$$\frac{\partial^2\Phi_{II}}{\partial^2 t} + g\frac{\partial\Phi_{II}}{\partial Z} = 0 \quad \text{on } S_{f2}$$
$$\nabla\Phi_{II} \to 0 \qquad \text{on } S_\infty \tag{5}$$
$$\Phi_{II} = \frac{\partial\Phi_{II}}{\partial t} = 0 \qquad \text{at } t = 0$$

The boundary integral equation of time domain Green function in the outer field II can be expressed as follows:

$$2\pi\Phi_{II} + \iint_{S_c} (\Phi_{II}G_n^0 - \Phi_{IIn}G^0)dS$$
$$= \int_0^t d\tau \left\{ \begin{array}{l} \iint_{S_c} (\Phi_{IIn}\tilde{G} - \Phi_{II}\tilde{G}_n)dS \\ +\dfrac{1}{g} \oiint_{w(\tau)} (\Phi_{II\tau}\tilde{G} - \Phi_{II}\tilde{G}_\tau)\vec{V}_N dl \end{array} \right\} \tag{6}$$

The continuity conditions on the control surface are the following:

$$\Phi_I = \Phi_{II}$$
$$\frac{\partial\Phi_I}{\partial n} = -\frac{\partial\Phi_{II}}{\partial n} \quad (\text{on } S_c) \tag{7}$$

Then, the fluid force F and moment M acting on the panel can be get by integrating the pressure obtained from Bernoulli`s equation along the wetted surface:

$$\vec{F} = \iint_{S_b} p\vec{n}dS$$
$$\vec{M} = \iint_{S_b} (\vec{r} \times \vec{n})pdS \tag{8}$$

where, $\vec{r}$, $\vec{n}$:the radial and normal vectors, defined in the ship-fixed coordinate system.

Viscous method

The internal force and moment due to the viscous flows of floodwater are given as:

$$\vec{F}^{In} = \int_S (\vec{f}_p + \vec{f}_s) \cdot \vec{n}dS$$
$$\vec{M}^{In} = \int_S \vec{r}_f \times (\vec{f}_p + \vec{f}_s) \cdot \vec{n}dS \tag{9}$$

Where, $\vec{f}_p$ and $\vec{f}_s$ are the pressure and shear force acting on the compartment wall, respectively. These forces calculated by commercial CFD software solving by the unsteady RANS (Reynolds time-averaged Navier-Stokes) equation with VOF (Volume of Fluid) multiphase flow model.

The governing equations of flow field include continuity equation, momentum equation and phase volume fraction equation are expressed as follows:

$$\begin{cases} \dfrac{\partial}{\partial t}\int_V \rho dV + \int_S \rho(\vec{u} - \vec{u}_g) \cdot \vec{n}dS = 0 \\ \dfrac{\partial}{\partial t}\int_V \rho\vec{u}dV + \int_S \rho\vec{u}(\vec{u} - \vec{u}_g) \cdot \vec{n}dS \\ +\int_V (\vec{\omega} \times \vec{u})dV = -\int_S p\vec{I}' \cdot \vec{n}dS \\ +\int_V \rho g dV + \int_S \mu(\nabla\vec{u} + \nabla\vec{u}^T) \cdot dS \\ \dfrac{\partial}{\partial t}\int_V \alpha dV + \int_S \alpha(\vec{u} - \vec{u}_g) \cdot \vec{n}dS = 0 \end{cases} \tag{10}$$

where, ρ: mixture density, can be defined as $\rho = \alpha\rho_w + (1-\alpha)\rho_g$, α: volume fraction of liquid phase, ρ_w, ρ_g: densities of liquids and gases, respectively; μ: average effective dynamic viscosity coefficient of phase volume fraction, in accordance with the definition of density; $\vec{u}$: the velocity of fluid micro-clusters; $\vec{u}_g$:the velocity of gird nodes; p: fluid pressure; $\vec{I}'$: the unit matrix; g: the acceleration of gravity; $\vec{\omega}$: the angular velocity of rotation. SST k-ω turbulent model is chosen for the closure of the equation.

In viscous flow calculations, motions of the internal compartment are determined by the translation velocity $\vec{u}_g(\dot{x}_i, i = 1..3)$ and angular velocity $\vec{\omega}(\dot{x}_i, i = 4..6)$ obtained by solving the equation (1). The momentum equation, turbulent kinetic energy k, dissipation rate ω or other transport equations are associated with volume fraction through density ρ and viscous coefficient μ in the whole viscous flow calculation region. Once the force and moment acting on the compartment wall are calculated they serve as initial condition for the next iteration of the equation (1).

Calculating Process

In the numerical simulation, the CFD method is only used to solve the floodwater motions and the resultant force acting on the compartment is applied to the ship's equations of motions in the time domain and the equations are solved by the potential theory solver. The inviscid flow solver can afford longer time steps because of the larger mesh size compared with viscous flow solver requiring shorter time steps. As a result it is necessary to introduce distinct time scales for CFD and inviscid solvers and use the

method of multi-step superposition. For example, if the time step associated with potential solver is given as Δt, then the viscous flow is solved in N inner time steps Δt_1 (where $\Delta t = N \Delta t_1$ and the value of N depends on the courant number). The floodwater forces after the N inner time steps is applied to the ship's equations of motion to ensure the unification of the two methods in calculation time. The calculation of damaged ship also need to consider the floodwater inflow and outflow the corresponding hydrodynamic force. This requires accurate calculation of the flowrates through the damaged opening and consequently a special boundary condition for the opening. This will be discussed in detail in the next section.

The calculation process of the unified viscous/potential prediction model is the following (Fig. 4):

(1) Initialization of ship motion by time domain potential flow solver, including initial time meshing and calculation of hydrodynamic coefficients;

(2) Initialization of the CFD flow field within damaged compartment, including the pressure and velocity fields, free surface, etc.

(3) The time-domain potential flow solver calculates the hydrodynamic and wave induced forces to solve the ship equations of motions. This steps involves also establishing of the boundary conditions of the flow field in the RANS solution, such as the boundary conditions of the computational domain or the damaged opening.

(4) The boundary conditions calculated by time domain potential method are transferred to CFD.

(5) After the boundary conditions are transferred to the viscous flow solver, it initializes the calculations of the floodwater ingress/egress and sloshing inside the damaged compartment. After a series of internal iterations, when the steady state is reached the solver computes the internal forces and moments due to floodwater flow and sloshing.

(6) The internal forces calculated by CFD are transferred to the time domain potential solver.

(7) The hydrodynamic loads due to floodwater are added to the external forces acting on the hull and the ship's equations of motions are solved by the fourth-order Runge-Kutta method.
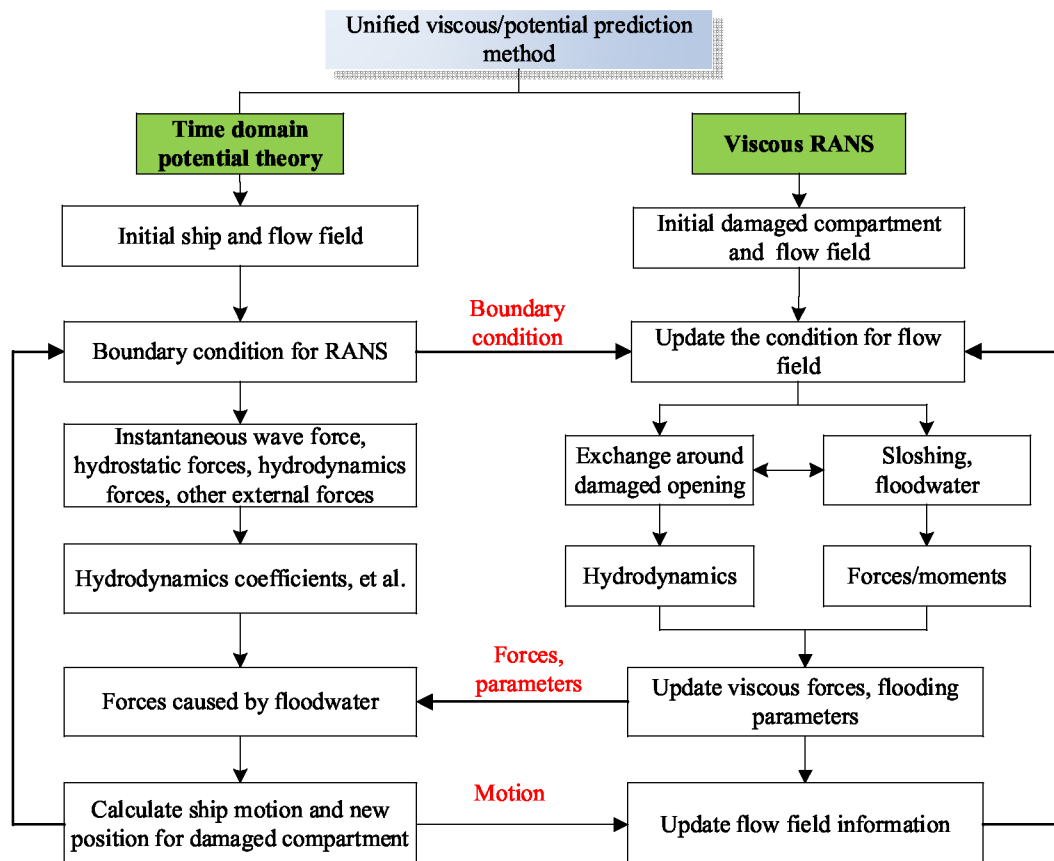

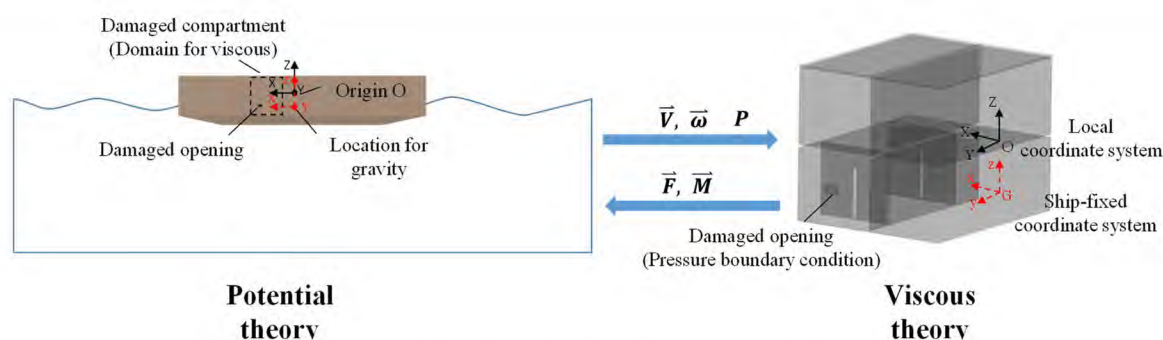Figure 4: Flow chart for calculation of unified viscous/potential prediction model

Figure 5: Diagram for the computing domain and coordinate systems

(8) The updated motions of the damaged compartment obtained from the inviscid solver are transferred to the CFD method.

(9) Repeat (3) - (8) until the calculation is completed.

The local coordinate system of the CFD solver is aligned with the inertial coordinate system used in the calculation of ship motions. As shown in Fig. 5, the force acting on the compartment is calculated based on the instantaneous position of the center of gravity.

Treatment for the damaged opening

The unified viscous/potential prediction model utilises three different methods for handling of the boundary condition at the damage openings:

(1) Far-field pressure boundary

The far field pressure boundary is applied to the domain constructed by constraining the entire CFD domain with two parallel planes aligned with the fore- and aft-most limits of the damaged compartments (Gao, et al., 2015). The front and back sections of the computational domain are slip wall boundary conditions while the upper and lower boundary conditions are far-field pressure boundary conditions. The corresponding pressure conditions are determined according to the position of the free surface. The interior and exterior walls of the compartment are the wall boundary conditions.

(2) Near-field pressure boundary

The idea of near-field pressure boundary originates from the observations made during CFD simulations, namely that the velocity field in the proximity of damage opening represents a "hemispherical" transition zone. Therefore, the computational domain consists of the interior region and a hemispherical region near the damage opening. The CFD solver does not need to set the free surface

position in this domain because there is no inconsistency of the free surface between viscous flow and potential flow.
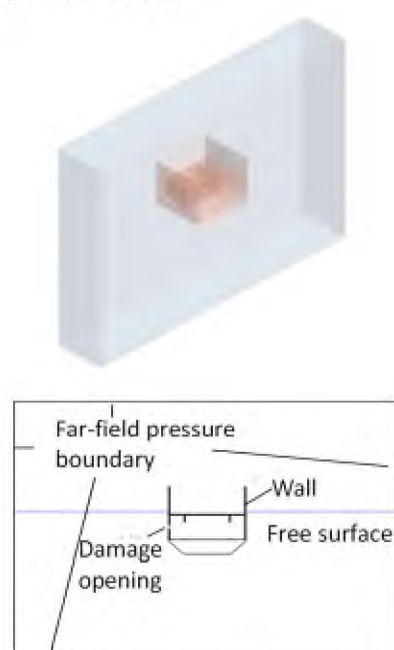

Figure 6: Diagram for the far-field pressure boundary

(3) Hatch pressure boundary

The idea of hatch pressure boundary stems from the problem of orifice and pipeline flow. The computational domain of this method includes only the interiors of the damaged compartment. The pressure inlet boundary condition at the damage opening is calculated by the potential solver. This coupling method has no external flow field and the flow into the compartment is entirely determined by the pressure applied at the damage opening. Therefore, in order to account for the influence of the floodwater flow, the hatch pressure needs to be corrected for the pressure loss, which is similar to the setting of the local pressure loss coefficient in the small outlet flow.
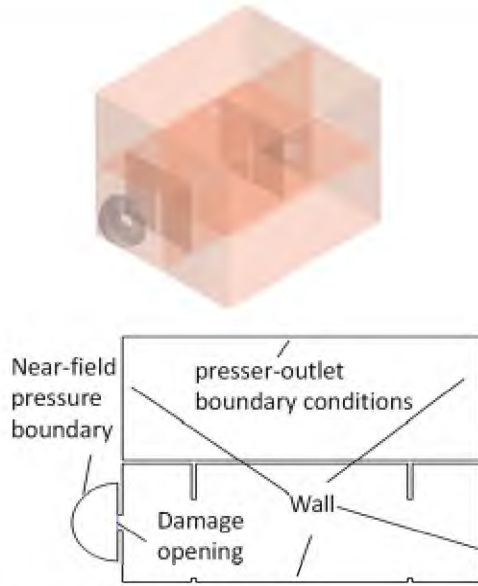
214

Figure 7: Diagram for the near-field pressure boundary
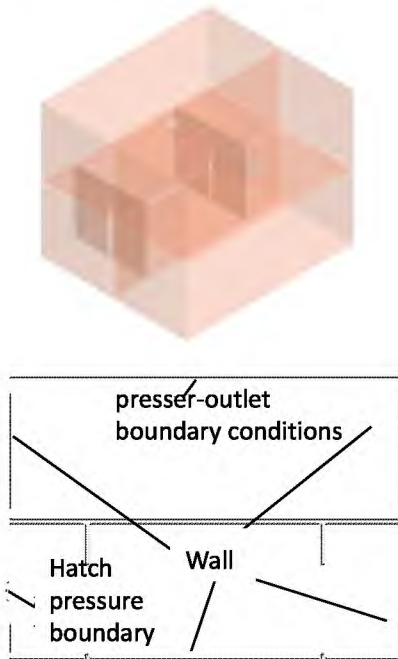

Figure 8: Diagram for the hatch pressure boundary

Herein, the hatch pressure boundary conditions in viscous flow calculations are given by modifying the hatch pressure obtained from potential flow calculation. Hence, pressure at the damage opening in CFD calculations is given as:

$$p_v = K \cdot p_0 \qquad (11)$$

where p_v is the pressure at the damage opening in CFD calculation; p_0 is the pressure near the damaged opening in potential flow calculation, including the first and second order pressure caused

by incident wave and disturbance potential; K is the local loss coefficient.

The results presented in this paper include the snapshots of velocity and pressure fields calculated by full CFD method, comparison of unified viscous/potential prediction model coupled with different boundary conditions at the damage opening (far-field pressure boundary, near-field pressure boundary and hatch pressure boundary condition). Initial value of the coefficient K is 0.6 and it increases gradually after 10s. Of course, further research is needed for the selection of the coefficient.
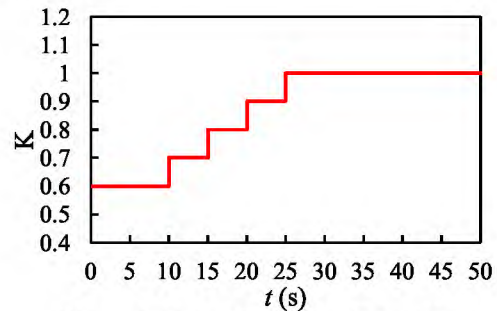

Figure 9: Values for the coefficient K.

4. RESULTS AND ANALYSIS

CFD simulation and validation

The dimensions of the computational domain are 15m×15m×10m. The meshing utilises the technique of overlapping grid. The wall boundary condition is used for the ship surface, and the pressure outlet condition is used for the external computational domain. There are two sets of grids in the computational domain (as shown in Fig. 10): background grid which contains the whole flow field and the overlapping grid containing the hull and the surrounding flow field. Data exchange between two sets of grids is carried out by interpolation near the interface. The total grids contain 1.3 million cells.

The calculations of floodwater levels in different compartments are in good agreement with model test results, as shown in Fig. 11, which validates the feasibility of the method.

Analysis of flowing process

In order to verify the reliability of the nonlinear time-domain unified viscous/potential prediction model presented in this paper, the numerical results calculated with different methods for handling boundary conditions at the damage opening, are compared with the experimental data.

215

The mesh quantity used for calculations are: 1.3 million cells for CFD simulation; 620,000 cells for unified prediction model with the far-field pressure boundary condition; 320,000 cells for unified prediction model with near-field pressure boundary condition and 300,000 for unified prediction model with hatch pressure boundary.

Fig. 12 shows the flow inside the compartment calculated with different methods. It can be seen from the figures that the transient inflow shows strong non-linear characteristics at t=5s. The near-field pressure boundary and hatch pressure boundary can better simulate the non-linear transient inflow than the far-field boundary condition. When t=25s, the floodwater begins to flow to the other side. The hatch pressure boundary offers the closest match to the calculation results of CFD simulation at this time instant. The far-field pressure boundary overestimated the inflow water, while the near-field pressure boundary proposed in this paper underestimated the inflow water. The inflow water is relatively small at this time, hence its impact on the ship behaviour may be relatively small. Overall, the three methods capture the flow process very well.

Fig. 13 shows the comparison of velocity fields calculated with different boundary conditions. It can be seen from the figures that, the near-field pressure boundary calculates the velocity field well, but the velocities calculated by the hatch pressure boundary are relatively small at t=5s. However, the accuracy become better with time. Overall, there is little difference in velocity fields calculated with the full CFD method, near-field pressure boundary, far-field pressure boundary and hatch pressure boundary which further validates the applicability of the boundary conditions in this problem.
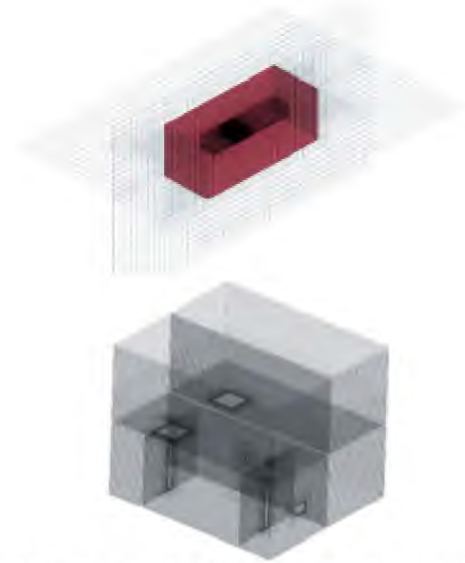

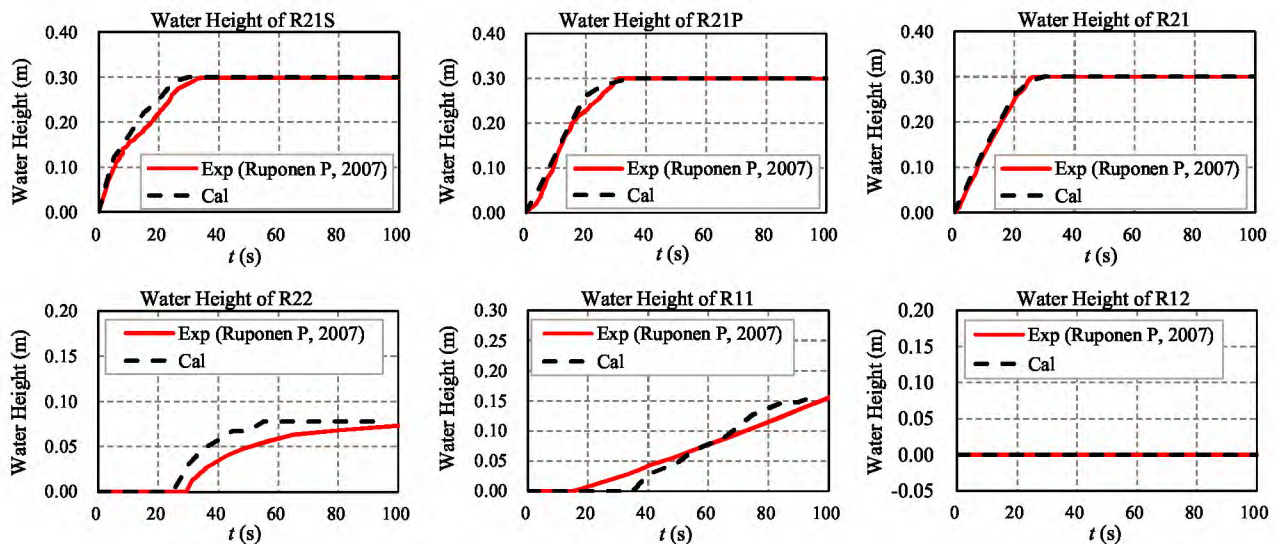Figure 10: Diagram for CFD computation domain and meshes

Figure 11: Comparisons of the variation of water level in different compartments
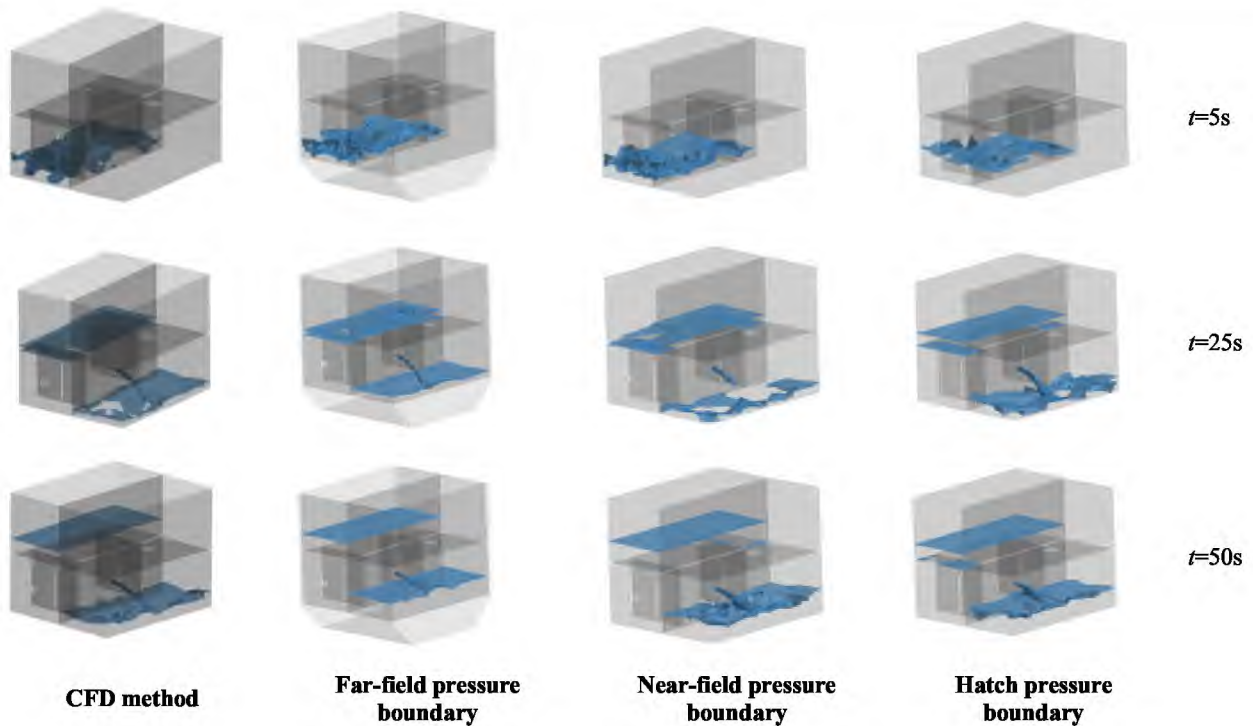
216

CFD method   Far-field pressure boundary   Near-field pressure boundary   Hatch pressure boundary

Figure 12: Flowing process calculated by different boundary conditions

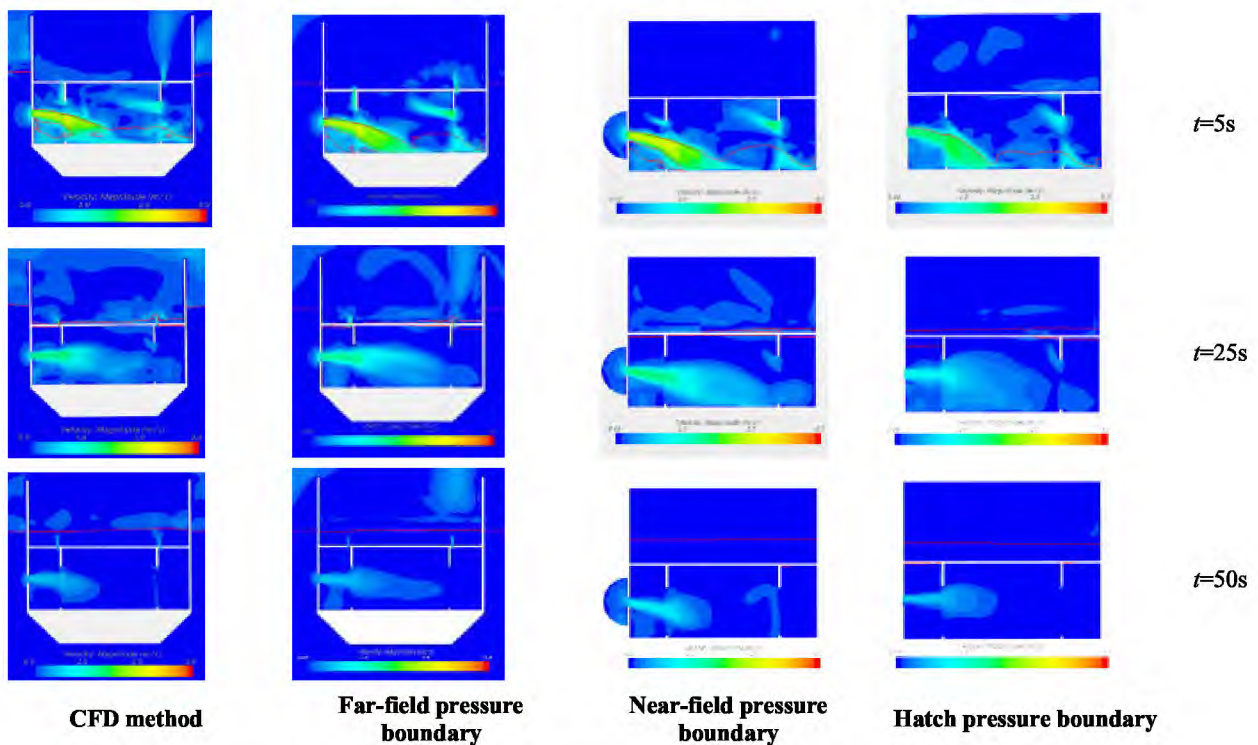CFD method   Far-field pressure boundary   Near-field pressure boundary   Hatch pressure boundary

Figure 13: Velocity contour of hatch section calculated by different boundary condition

Analysis of damaged ship motion

The results of unified viscous/potential prediction model, CFD simulations and model test are compared in Fig. 14.

For the roll motion, the errors by hatch pressure boundary at the initial stage are relatively large, possibly caused by the errors in calculations of floodwater inflow, roll damping, etc, and can be neglected. For the heave and pitch motions, the calculated results of CFD simulation, far field pressure boundary, near field pressure boundary and hatch pressure boundary are all in good agreement with the model tests.

217

The comparison of the time-domain motions calculated by unified viscous/potential prediction model with different methods for handling of boundary conditions prove that CFD, the near-field pressure boundary and hatch pressure boundary proposed in this paper can calculate motions of the damaged ship well.

Considering that the calculation of far-field pressure boundary needs to include a relatively large computational domain outside the damaged opening, the mesh quantity is much larger than that of near-field boundary conditions and hatch pressure boundary conditions. Furthermore, there exists a problem of inconsistency between the potential and viscous solutions in the calculation of wave conditions under far-field boundary conditions, especially when the incoming flow is parallel or intersecting with the damaged opening. The near-field pressure boundary and hatch pressure boundary on the other hand, can be used to calculate damaged ship motion under different wave directions and ship speeds.
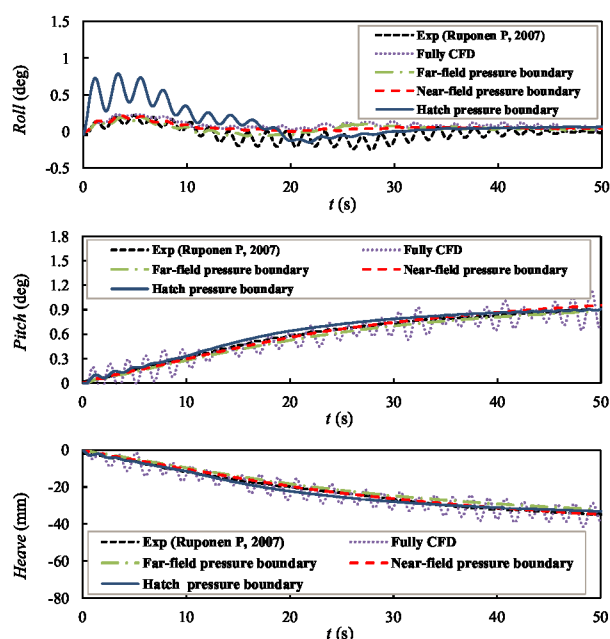

Figure 14: Time history of motions calculated by different methods

5. CONCLUSION

In this paper, a unified viscous/potential prediction model for stability in waves is proposed based on the real-time interactive iteration of three dimensional time domain hybrid source method and viscous CFD method. The unified model combines the advantages of the three dimensional time domain hybrid source method in calculating extreme motions of ships in waves, and the advantages of CFD method in detailed simulations for hull-floodwater interactions. Two time scales, fast scale and slow scale, are introduced and two boundary condition forms for damage opening in the unified model are also proposed. The research and analysis show that:

(1) The unified viscous/potential prediction model established in this paper can be effectively applied to the study of real-time coupled damaged flow of damaged ships.

(2) The comparisons of flow process, velocity, pressure with full CFD method and model tests verify the effectiveness of the proposed unified viscous/potential prediction model for the prediction of damaged ships stability in waves.

(3) The proposed near-field pressure boundary and hatch pressure boundary for the damaged opening can significantly reduce mesh quantity and improve computation efficiency without compromising the accuracy of calculations.

6. ACKNOWLEDGEMENTS

7. REFERENCES

Bu S, Gu M, Lu J, Zeng K. Time domain prediction of the damaged ship motion in waves [J]. Shipbuilding of China [J]. 2018, 59(2): 80-80.

Bu S, Gu M, Lu J, Abdel-Maksoud M, Effects of radiation and diffraction forces on the prediction of parametric roll [J], Ocean Engineering. 175(2019a):262-272

Bu S, Gu M, Abdel-Maksoud M. Study on roll restoring arm variation using a three-dimensional hybrid panel method [J], Journal of Ship Research. 2019b,

https://doi.org/10.5957/JOSR.09180078

Cho S K, Hong S Y, Kyoung J H. The numerical study on the coupled dynamics of ship motion and flooding water[C]// Proc. 9th STAB, Rio de Janeiro, Brazil, 2006:599-605.

Chang B C, Blume P. Survivability of damaged Ro-Ro passenger vessels-ship technology research [J]. Schiffstechnik, 1998, 45(3): 105-117.

Gao Q, Vassalos D. The dynamics of the floodwater and the damaged ship in waves [J]. Journal of Hydrodynamics, 2015, 27(5): 689-695.

Gao Z, Gao Q, Vassalos D. Numerical simulation of flooding of a damaged ship [J]. Ocean Engineering, 2011, 38(14): 1649-1662.

Gao Z, Gao Q, Vassalos D. Numerical study of damaged ship flooding in beam seas [J]. Ocean Engineering, 2013, (61): 77-87.

Hashimoto H, Kawamura K, Sueyoshi M. Numerical simulation of ship transient behavior coupled with water flooding [C]// Proc. 25th ISOPE, Koan, USA. 2015:1251-1258.

ITTC. Final report and recommendation to the 24th ITTC [R]. The specialist committee on stability in waves, 2005 (II): 369-408.

Jasionowski A, Vassalos D. Numerical modelling of damage ship stability in waves[C]//5th International Workshop on Stability and Operational Safety of Ships, Trieste, 2001:7.3.1-7.3.7

Nabavi Y, Calisal S M, Akinturk A, et al. A computational investigation of the three dimensional geometric parameters' effects on the discharge rate of a ship opening [C]// Proc. 9th STAB, Rio de Janeiro, Brazil, 2006: 617–624.

Ruponen P, Sundell T, Larmela M. Validation of a simulation method for progressive flooding [J]. International Shipbuilding Progress, 2007, 45:305-321.

Spanos D, Papanikolaou A. On the time to capsize of a damaged RoRo/passenger ship in waves[C]//Proc. 9th ISSW, Germany. 2007.

Santos T A, Guedes Soares C. Study of the dynamics of a damaged passenger Ro-Ro ship[C]//Proc. 9th STAB, Rio de Janeiro, Brazil, 2006: 25-29.

Santos T A, Soares C G. Study of damaged ship motions taking into account floodwater dynamics [J]. Journal of Marine Science and Technology, 2008, 13(3): 291-307.

Strasser C. Simulation of Progressive Flooding of Damaged Ship by CFD [D]. Ph.D. Thesis. Universities of Glasgow and Strathclyde, 2010.

Umeda N, Kamo T, Ikeda Y. Some remarks on theoretical modeling of damaged stability [J]. Marine Technology, 41(1), 2004:45-49.

Van Walree F, de Kat J O, Ractliffe A T. Forensic research into the loss of ships by means of a time domain simulation tool [J]. International Shipbuilding Progress, 2007, 54(4): 381-407.